

Turbostratic graphene formation by flash joule heating: a comprehensive characterization study

Ulya Saffanah^{1,3}, Winona Avis^{2,3}, Hendri Widiyandari^{2,3}, Endah Retno Dyartanti^{1,3}, and Agus Purwanto^{1,3*}

¹ Department of Chemical Engineering, Faculty of Engineering, Sebelas Maret University, Surakarta, Indonesia

² Department of Physics, Faculty of Mathematics and Natural Sciences, Sebelas Maret University, Surakarta, Indonesia

³ Center of Excellence for Electrical Energy Storage Technology, Sebelas Maret University, Surakarta, 57146, Indonesia

Abstract. Graphene is a technologically important two-dimensional carbon material due to its exceptional electrical conductivity, mechanical strength, and potential for energy storage applications. However, conventional graphene synthesis methods often encounter challenges related to scalability, structural control, and environmental sustainability. Flash Joule Heating (FJH) provides an alternative approach that enables high-temperature conversion of carbon-based materials through a simplified process. In this study, turbostratic graphene was synthesized from a mixture of commercial graphite and acetylene black (AB) using FJH method. Raman spectroscopy revealed an increased intensity ratio of the D to G band I_D/I_G indicating a higher density of structural defects, while the intensity ratio of the 2D to G band I_{2D}/I_G confirmed the presence of few-layer graphene. X-ray diffraction (XRD) analysis showed rotational disorder of graphene layers, characteristic of turbostratic stacking. While Scanning Electron Microscopy (SEM) images revealed the transformation of compact graphite particles into fractured and thinner structures. The addition of AB increased defect density and influenced the structural and electrical-related properties of the resulting material. These results demonstrate that FJH enables the direct conversion of commercial graphite into turbostratic graphene through an efficient and environmentally sustainable route with promising potential for energy storage applications.

1 Introduction

Graphene is a two-dimensional carbon allotrope composed of sp^2 -hybridized carbon atoms arranged in a hexagonal lattice. Graphene exhibits exceptional mechanical, electrical, and thermal properties arising from its two-dimensional sp^2 -bonded carbon structure, making it an attractive material for a wide range of advanced applications. These properties have driven

*Corresponding author: aguspurwanto@staff.uns.ac.id

extensive research into graphene-based materials for electronic, optoelectronic, and energy-related devices [1].

Structurally, graphene is derived from graphite, a layered carbon material composed of stacked graphene sheets [2]. Consequently, graphite is a natural and widely used precursor for graphene production through top-down approaches. Graphite has a non-equivalent layer arrangement, called A and B in Bernal configuration (ABABAB...). The interlayer spacing in graphite is approximately 3.35 Å, while the in-plane carbon-carbon σ bonds have a bond length of about 1.42 Å. The remaining p orbitals form delocalized π bonds oriented perpendicular to the basal plane, leading to weak interlayer attraction between adjacent graphene layers [3]. Currently, the anode material of lithium ion batteries is based on graphite because it has good stability, high coulomb efficiency, affordable, safe, and good cycling performance. Graphite has a maximum theoretical Li^+ storage capacity of 375 mAh g^{-1} [4]. Many studies have been explored to improve the electrochemical performance of graphite anodes, such as the use of smaller particles, preparing graphite/nano-powder composites, and oxidizing or purifying graphite [5]. In addition, acetylene black (AB) is a conductive carbon material with an amorphous to partially graphitized structure. AB is another carbon allotrope which is formed through carbon derived from an incomplete combustion of acetylene gas (C_2H_2) under a controlled temperature and pressure without the presence of oxygen. AB has several advantages, including conductive properties in charge transfer, high porosity and surface area with a good absorptivity and chemically stable [6]. Due to its high electrical conductivity, surface area, and structural compatibility with graphitic carbon, AB is commonly used as a conductive additive in lithium-ion battery electrodes and can influence electrical and structural evolution during high-temperature processes.

Graphene synthesis is commonly divided into two main approaches based on the type of starting material. In the top-down approach, graphite is used as the precursor and the process aims to weaken the interactions between graphene layers so that thinner sheets can be obtained. By contrast, the bottom-up approach starts from various carbon-based precursors, which are broken down under high-energy conditions, allowing carbon atoms to rearrange and form graphene [7]. However, existing synthesis methods have several deficiencies, including time efficiency, inconsistent final product results, using chemicals that causes potential to damage the environment. To improve these shortcomings, the flash joule heating method offers advantages in terms of time efficiency and eco-friendly.

Flash joule heating (FJH) is a synthesis method used to convert carbon precursors into graphene. In this process, electrical energy stored in capacitors is rapidly released into the precursor material, producing intense Joule heating within a millisecond. The discharge generates a high current (>400 A) at low voltage, leading to a short thermal pulse with temperatures reaching approximately 3000 K. Such ultrafast heating enables rapid structural transformation of carbon materials without extended thermal treatment. As a result, FJH is considered a promising approach for high-temperature material synthesis due to its simplicity and short processing time [8]. During FJH, the electrical conductivity of the precursor mixture affects the current distribution and heat generation within the system. In this study, AB is used not only as a conductive additive but also as a variable to control the conductivity of the precursor mixture. Variation of the AB content is expected to influence the FJH process and the resulting structural transformation of graphite into turbostratic graphene. The resulting FJH-treated materials are subsequently utilized as conductive additives in graphite-based anodes to evaluate their effect on the electrochemical performance of lithium-ion batteries.

A comparison of commonly reported graphene synthesis methods, including their raw materials, advantages, and limitations, is summarized in Table 1. Although various top-down and bottom-up approaches have been explored, many methods remain limited by complex processing steps, low scalability, or environmental concerns.

Most studies have used polymeric or waste-derived carbon precursors. This work investigates acetylene black as a conductive additive in the FJH of commercial graphite and its effect on the resulting turbostratic structure.

Table 1. Variations of graphene synthesis methods [7]

Raw material	Method	Result	Advantage	Disadvantage
Graphite	Hummers, modified hummers, improved hummers	Graphene oxide (GO)	- Higher reaction efficiency and safer operating conditions than Brodie and Staudenmaier methods - Tunable physical and electrochemical properties through synthesis parameter control	- Oxidation step produces toxic gases (NO ₂ and N ₂ O ₄) - Residual Na ⁺ and NO ₃ ⁻ ions are difficult to remove from wastewater after GO synthesis and purification
CH ₄ , C ₂ H ₆ , C ₃ H ₈ gas/ SiC	Epitaxial growth on SiC	Graphene	Precise control over graphene layer thickness	Limited scalability
CH ₄ , C ₂ H ₆ , C ₃ H ₈ gas/ SiC	Chemical vapor deposition	Graphene	High-quality graphene with large domain size	High production cost and complex process control
CH ₄ , C ₂ H ₆ , C ₃ H ₈ gas/ SiC	Arc discharge method	Graphene	Relatively high production rate	Carbonaceous impurities
Graphite	Mechanical/ Micromechanical exfoliation	Graphene	Large graphene flakes with minimal structural defects	Limited scalability
Graphite	Chemical synthesis	Reduced graphene oxide (rGO)	Scalable and low-cost process	Low yield and requires additional purification
Graphite	Liquid phase exfoliation	Graphene	High-quality graphene with relatively low defect density	- Limited availability of suitable solvents - Dependence on costly and potentially toxic dispersing solvent

2 Material and Method

2.1 Material

The materials used in this research include graphite powder (Gelon LIB. Co. Ltd., China), acetylene black (AB) (Gelon LIB. Co. Ltd., China), distilled water, and copper foil. All materials were used as received without further purification.

2.2 Preparation and application of the FJH method

Four samples were prepared to investigate the effects of the FJH method with varying AB contents. Untreated commercial graphite was used as the control sample (Gft). The remaining samples consisted of commercial graphite mixed with different weight percentages AB, namely FG-5 (5 wt% AB), FG-10 (10 wt% AB), and FG-15 (15 wt% AB), which were synthesized using FJH method to evaluate the influence of AB concentration on the structural properties of the resulting materials. For each experiment, 0.4 g of sample was placed in a quartz tube and compressed between a copper foil and a copper rod electrode to ensure effective electrical contact. The FJH system employed a capacitor bank composed of ten capacitors, each with a capacitance of 6 mF. The capacitor bank was charged to approximately 400 V, as monitored using a multimeter, and subsequently discharged ten times under identical electrical conditions for all FJH-treated samples. The FJH process generated extreme thermal gradients, leading to rapid structural transformation of the carbon materials. All experiments were conducted under ambient atmospheric conditions. After the discharge sequence, the samples were allowed to cool naturally to room temperature before further characterization. The energy released during the FJH process can be controlled by adjusting the effective capacitance while operating under identical voltage and discharge conditions. The energy associated with the capacitor discharge is described by Equation (1):

$$E = (V_1^2 - V_2^2) \times \frac{C}{2} \times M \quad (1)$$

Where E refers to the energy consumed during the reaction (J), V_1 and V_2 denote the capacitor voltages before and after discharge, respectively, C represents the capacitance of the capacitor (F), and M corresponds to the mass of the processed material (g) [9].

Lithium-ion battery electrodes were prepared using graphite, acetylene black (AB), FG-10, carboxymethyl cellulose (CMC), styrene butadiene rubber (SBR), and a 1 M lithium hexafluorophosphate (LiPF_6) electrolyte dissolved in a mixed ethylene carbonate/dimethyl carbonate (EC/DMC) solvent (Gelon LIB Co., Ltd., China). The powders, including graphite, AB, and FG-10, were dispersed into an aqueous CMC solution and mechanically stirred at a constant speed of 1000 rpm for three hours to obtain a homogeneous slurry. The mass ratio of graphite, FG-10, AB, CMC, and SBR was maintained at 83:7:1:3:6 wt%, respectively. The resulting slurry was then coated onto copper foil using a doctor blade with a preset thickness of 200 μm . Coin-type half-cells (CR2032) were assembled with lithium metal as the counter electrode and evaluated using a NEWARE battery testing system controlled by the BTS software. Electrochemical measurements were conducted within a voltage window of 0.1-1.5 V to investigate the specific capacity, cycling stability, and rate performance of the cells.

3 Results and Discussion

3.1 Raman Spectroscopy

Raman spectroscopy was used to evaluate the structural quality of graphene and other carbon materials. In graphene, three prominent peaks were observed, corresponding to the D ($\sim 1350 \text{ cm}^{-1}$), G (1580 cm^{-1}), and 2D (2700 cm^{-1}) bands [9]. The G band resulted from the in-plane vibrations of sp^2 -bonded carbon atoms, whereas the D band was caused by out-of-plane vibrations associated with structural defects. The defect level in the carbon structure was evaluated using the intensity ratio of the D band to the G band (I_D/I_G). A smaller I_D/I_G ratio

corresponded to a lower defect level, whereas a higher ratio reflected greater structural disorder.

Based on the raman spectroscopy characterization results, the I_D/I_G ratio value of the Gft sample is 0.14. The level of defects or defects in graphite (Gft) is low as evidenced by the low intensity of the D band in Figure. Graphite has a very good regularity of atomic arrangement which leads to low structural defects in the graphite arrangement. Samples FG-5, FG-10, and FG-15 have I_D/I_G ratio values of 0.27; 0.59; 0.42, respectively. Based on Farivar et al. [10] graphite material has the smallest I_D/I_G ratio value when compared to other carbon derivatives, which has the I_D/I_G ratio <0.1 , while the graphene sample ratio value ranges from 0.19-0.33, which shows that graphene has a defects are higher compared to graphite because it undergoes a exfoliation process. Samples that have been synthesized using the FJH method have a higher level of defects than the Gft samples. This increase in D band intensity indicates defect generation induced by extreme thermal gradients and rapid quenching during the FJH process. The effect of this heating can break the carbon bonds in the graphite array, causing defects in the flash graphene material.

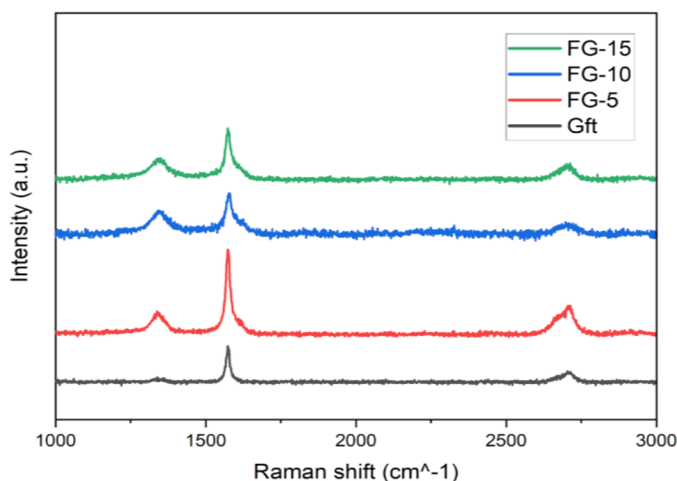


Fig. 1. Result of raman spectroscopy characterization for each variation.

In general, the I_{2D}/I_G ratio in graphene serves as a key indicator of layer thickness. An I_{2D}/I_G ratio greater than 2 indicates single-layer graphene, while ratios between 1 and 2 indicate bilayer graphene. Ratios below 1 are diagnostic of few-layer graphene (more than two layers) [11]. Our Raman spectral analysis revealed I_{2D}/I_G ratios of 0.34; 0.31; and 0.32 for samples FG-5, FG-10, and FG-15, respectively. The consistently low ratios (<1) and the 2D band profiles confirm that the synthesized graphene consists of more than two layers, classifying it as few-layer graphene. Although increased defect density is often associated with structural disorder, such defects may be beneficial for electrochemical applications by providing additional active sites and facilitating ion diffusion pathways. The observed defects are likely associated with edge-related and basal-plane disorder resulting from rapid thermal expansion and quenching, consistent with previously reported FJH-derived graphene materials.

3.2 X-ray Diffraction (XRD)

XRD characterization was used to determine the crystal phase formed in the flash graphene sample through the diffraction peaks produced. The analysis was carried out in the range of

$2\theta = 10^\circ$ - 60° and $2\theta = 40^\circ$ - 70° so that the data generated was more focused and the 2θ angle peak did not widen. The diffraction pattern that appeared on the Gft sample was located at peak (002) with a value of $2\theta = 26.4$; peak (101) with a value of $2\theta = 44.4$; and peak (004) with a value of $2\theta = 55.4$. Each has an inter-plane distance (d_{hkl}) of 3.37 Å, 2 Å, and 1.7 Å.

Based on the results of XRD characterization, it could be seen in Figure 2(a) that the diffraction pattern of each sample showed a peak (002) at a diffraction angle of $2\theta = 26.4^\circ$ with decreasing intensity in each sample variation. The strongest diffraction peak was found in the Gft sample. The drastic decrease in intensity in the (002) plane in the flash graphene samples formed was due to defects in the carbon arrangement and a decrease in crystal size.

High irregularity due to defects in sp^2 hybridization in the graphene layer can cause a decrease in the degree of graphitization in the carbon array formed. This is supported by the research of Badri et al. [12] which showed a drastic decrease in the intensity of peak (002) in exfoliated graphene material caused by a decrease in graphite thickness due to the rupture of inter-planar carbon in the graphite structure. In this study, cracked carbon atoms in graphite were caused by the combustion reaction generated during the FJH process. The intensity of the diffraction peak in the (002) plane decreases with the addition of Acetylene Black (AB). The decreasing intensity indicates that the crystal size is getting smaller. Very small crystals will produce wide diffraction peaks because small crystallinity has a limited x-ray reflection field. The smaller the crystal size of a material, the greater the FWHM and the intensity peak decreases [13].

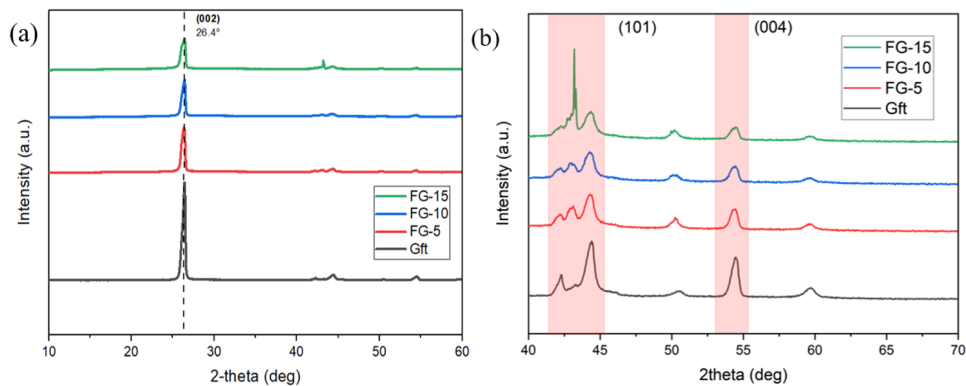


Fig. 2. XRD characterization results of each variation at diffraction angle (a) $2\theta = 10^\circ$ - 60° (b) $2\theta = 40^\circ$ - 70° .

X-ray Diffraction (XRD) in addition to being used to analyze the crystal structure can also be used to analyze the stack of graphene sheets [9]. In Figure 2(b) it could be seen that the peak (101) at a diffraction angle of $2\theta \sim 44.4^\circ$ in each sample variation decreases when compared to the Gft sample. It can also be seen that at this diffraction angle, the peak shifted towards a smaller angle, especially in sample FG-15, the diffraction angle shifts at $2\theta \sim 43.2^\circ$.

In addition, there is also a peak (004) at a diffraction angle of $2\theta \sim 55.4^\circ$. The intensity of the peak at the diffraction angle was also seen to decrease in each sample variation when compared to the Gft sample. The peaks that appear in the (101) and (004) planes are 3-dimensional lines. If the intensity of the 3-dimensional lines decreases, it indicates the rotation of the graphene layer [9]. Sample variations FG-5, FG-10, FG-15 each experienced rotation of the graphene layer as a result of the FJH method applied to the sample. The (004) plane is affected due to a change in the arrangement of carbon atoms after undergoing the heating process. Line (001) shifts to a lower diffraction angle, while the intensity of other three-dimensional lines (hkl) decreases. The carbon atoms in the graphene layer may deviate

along the graphene normal layer from their usual positions due to compaction resulting from the FJH process. The fluctuation of atomic positions along the graphene layer normal line has a strong influence on the intensity of line (00l) [14]. Therefore, the graphene layer formed is turbostratic. In this study, the formed sample is referred to as turbostratic flash graphene (tFG) because in the process it undergoes structural changes due to the FJH method.

3.3 Scanning Electron Microscope (SEM)

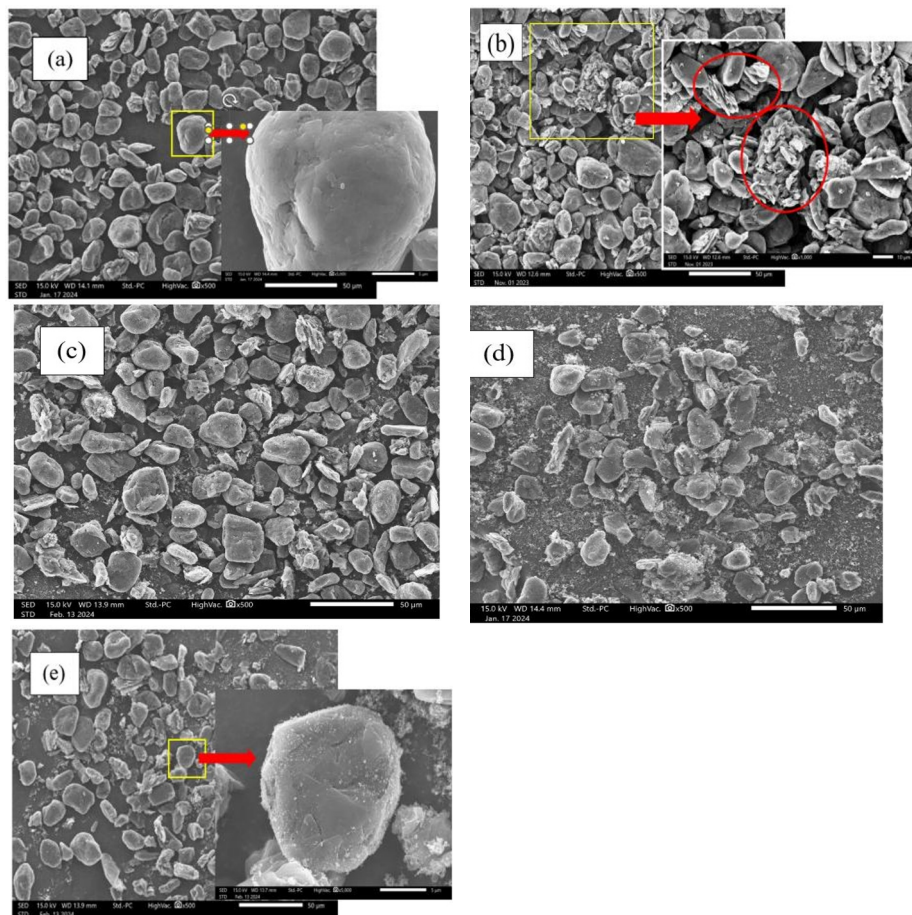


Fig. 3. Morphology of (a) graphite (Gft), (b) graphite after FJH treatment without AB, and FJH-treated graphite with AB contents of (c) 5 wt% (FG-5), (d) 10 wt% (FG-10), and (e) 15 wt% (FG-15).

The morphology of the pristine graphite (Gft) was characterized by compact, block-like particles with relatively smooth surfaces, as shown in Figure 3(a). This morphology reflects the highly ordered and densely stacked structure of untreated graphite, where individual graphene layers are strongly held together by van der Waals interactions. After treatment using the FJH method, significant morphological changes were observed. As presented in Figure 3(b), the graphite particles exhibited pronounced fragmentation, with the original large agglomerates breaking into smaller and irregularly shaped particles. In addition, portions of the fractured particles display thinner, sheet-like features, indicating partial exfoliation induced by the ultrafast thermal shock during the FJH process. These morphological changes were attributed to the FJH process and subsequent quenching, which generated extreme thermal gradients capable of disrupting the interlayer interactions within

graphite. Figures 3(c)-3(e) show the morphology of FJH-treated graphite with different acetylene black (AB) contents (5 wt%, 10 wt%, and 15 wt%). All AB-containing samples exhibited similar fragmentation and surface roughening, suggesting that the presence of AB does not alter the overall exfoliation pattern but may influence the extent and uniformity of the structural transformation. In particular, finer particulate features with a sand-like appearance are observed surrounding the graphite fragments, which were attributed to the dispersed AB particles.

The incorporation of AB is expected to enhance the electrical conductivity of the precursor mixture, thereby promoting more homogeneous current distribution and heat generation during FJH, which in turn facilitates more effective graphite fragmentation and exfoliation. The observed reduction in particle size and emergence of thinner structures qualitatively support the structural disorder and turbostratic characteristics inferred from Raman spectroscopy and XRD analyses. Based on the characterization results, FG-10 was used as the representative FJH-treated sample for electrochemical evaluation because it represents an intermediate AB content (10 wt%), which is expected to provide a balanced composition for effective structural transformation during the FJH process. Therefore, only FG-10 was incorporated as a conductive additive in the graphite anode to investigate its influence on the electrochemical performance of the assembled coin cell.

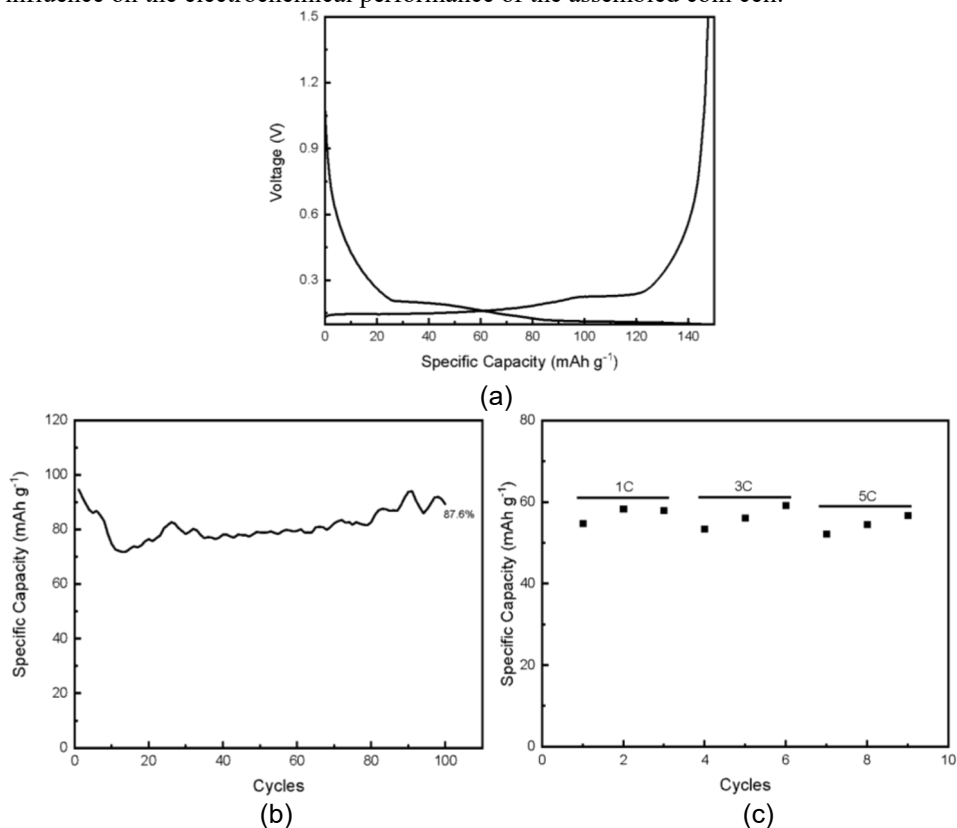


Fig 4. Electrochemical performance test of FG-graphite: a. voltage profile charging-discharging, b. Cycling test standard condition, c. Rate ability test.

The (FG-10)-graphite (FG-graphite) coin cell was assembled using an anode formulation consisting of graphite, FG-10, AB, CMC, and SBR with mass fractions of 83, 7, 1, 3, and 6 wt%, respectively. The electrochemical behaviour of the FG-graphite cell was evaluated through galvanostatic charge-discharge measurements. As shown in Figure 4a, the initial

discharge capacity of the FG-graphite electrode reached 145.2 mAh g⁻¹. The cycling performance and rate capability are presented in Figure 4b and 4c. Cycling stability was evaluated at a charge current of 0.5C and a discharge current of 1C. As illustrated in Figure 4b, the cell maintained 87.6% of its initial capacity after 100 cycles, demonstrating that the presence of FG-10 effectively enhances capacity retention and cycling stability. Furthermore, the rate performance test (Figure 4c) was conducted over a range of charge rates from 1C to 5C, while the discharge current was fixed at 0.5C. The results indicate that even at a high charge rate of 5C, the specific capacity decreased by only 0.4% relative to the initial cycle. This behaviour suggests that the incorporation of FG-10 into the graphite anode promotes improved electronic conductivity and facilitates lithium-ion transport, leading to enhanced rate capability.

4 Conclusion

Turbostratic graphene was successfully synthesized from commercial graphite mixed with acetylene black (AB) using the flash Joule heating (FJH) method. Raman spectroscopy revealed an increased defect density, while XRD analysis confirmed the presence of rotational disorder characteristic of turbostratic stacking. SEM observations further demonstrated the transformation of compact graphite particles into fractured and thinner structures after FJH treatment. The FJH method offers notable advantages, including rapid processing, solvent-free synthesis, and scalability. When applied as a conductive additive in graphite-based anodes, the FJH-derived material (FG-10) exhibited promising electrochemical performance. The FG-graphite coin cell delivered an initial discharge capacity of 145.2 mAh g⁻¹ and maintained stable rate capability, with only a 0.4% capacity reduction at a high charge rate of 5C. Moreover, the cell retained 87.6% of its initial capacity after 100 cycles, indicating enhanced rate capability and cycling stability. These results demonstrate that the incorporation of turbostratic graphene can facilitate electronic conductivity and lithium-ion transport within the anode. Further optimization of defect density and AB content is required to fully realize its potential for lithium-ion battery applications.

This research is supported by research scheme for Research Group Capacity Strengthening (PKGR-UNS) B (Grant Number: 371/UN27.22/PT.01.03/2025) and the Center for Excellence in Electrical Energy Storage Technology of Sebelas Maret University as a facility provider.

References

- [1] F. Bonaccorso, A. Lombardo, T. Hasan, Z. Sun, L. Colombo, and A. C. Ferrari, "Production and processing of graphene and 2d crystals," *Materials Today*, vol. 15, no. 12, pp. 564–589, 2012, doi: 10.1016/S1369-7021(13)70014-2.
- [2] M. S. Seehra, U. K. Geddam, D. Schwegler-Berry, and A. B. Stefaniak, "Detection and quantification of 2H and 3R phases in commercial graphene-based materials," *Carbon N. Y.*, vol. 95, pp. 818–823, 2015, doi: 10.1016/j.carbon.2015.08.109.
- [3] P. Mukhopadhyay and R. K. Gupta, *Graphite, graphene, and their polymer nanocomposites*. Boca Raton: CRC Press, 2012. doi: 10.1201/b13051.
- [4] M. Mottaghi and J. M. Pearce, "A Review of 3D Printing Batteries," *Batteries*, vol. 10, no. 3, 2024, doi: 10.3390/batteries10030110.
- [5] C. Wang, H. Zhao, J. Wang, J. Wang, and P. Lv, "Electrochemical performance of modified artificial graphite as anode material for lithium ion batteries," *Ionics (Kiel)*, vol. 19, no. 2, pp. 221–226, 2013, doi: 10.1007/s11581-012-0733-9.

- [6] R. da Silva, L. G. da Silva Catunda, and R. M. Buoro, "Multiple comparisons of acetylene black-based rigid composite electrodes: comprehensive evaluation of chemical properties and electrochemical sensing potentialities," *Journal of Solid State Electrochemistry*, no. 0123456789, 2024, doi: 10.1007/s10008-024-06012-3.
- [7] K. Edward, K. Mamun, S. Narayan, M. Assaf, D. Rohindra, and U. Rathnayake, "State-of-the-Art Graphene Synthesis Methods and Environmental Concerns," *Appl. Environ. Soil Sci.*, vol. 2023, no. ii, 2023, doi: 10.1155/2023/8475504.
- [8] S. Dong *et al.*, "Ultra-fast, low-cost, and green regeneration of graphite anode using flash joule heating method," *EcoMat*, vol. 4, no. 5, pp. 1–10, 2022, doi: 10.1002/eom2.12212.
- [9] P. A. Advincula, D. X. Luong, W. Chen, S. Raghuraman, R. Shahsavari, and J. M. Tour, "Flash graphene from rubber waste," *Carbon N. Y.*, vol. 178, pp. 649–656, 2021, doi: 10.1016/j.carbon.2021.03.020.
- [10] F. Farivar, P. L. Yap, R. U. Karunagaran, and D. Losic, "Effect of Particle Size of Graphene, Graphene Oxide and," *Journal of Carbon Research*, vol. 7, p. 41, 2021.
- [11] U. Mogera, R. Dhanya, R. Pujar, C. Narayana, and G. U. Kulkarni, "Highly Decoupled Graphene Multilayers: Turbostraticity at its Best," *Journal of Physical Chemistry Letters*, vol. 6, no. 21, pp. 4437–4443, 2015, doi: 10.1021/acs.jpcclett.5b02145.
- [12] M. A. Saiful Badri, M. M. Salleh, N. F. ain Md Noor, M. Y. A. Rahman, and A. A. Umar, "Green synthesis of few-layered graphene from aqueous processed graphite exfoliation for graphene thin film preparation," *Mater. Chem. Phys.*, vol. 193, pp. 212–219, 2017, doi: 10.1016/j.matchemphys.2017.02.029.
- [13] A. Balfas, S. Nikmatin, and A. Sukarto, "Milling effect towards nanoparticle biomass rattan characteristics," *Jurnal Keteknikan Pertanian*, vol. 04, no. 1, pp. 81–86, 2016, doi: 10.19028/jtep.04.1.81-86.
- [14] Z. Q. Li, C. J. Lu, Z. P. Xia, Y. Zhou, and Z. Luo, "X-ray diffraction patterns of graphite and turbostratic carbon," *Carbon N. Y.*, vol. 45, no. 8, pp. 1686–1695, 2007, doi: 10.1016/j.carbon.2007.03.038.